

Near Source Affects and Engineering Observations of M_w 6.1 February 22, 2011 Christchurch, New Zealand Earthquake



C. A. Davis and J. Hu

Los Angeles Department of Water and Power, Los Angeles, CA, USA

SUMMARY:

The M_w 6.1 (USGS) February 22, 2011 Christchurch earthquake caused much greater damage in Christchurch than the nearby M_w 7.0 (USGS) September 4, 2010 Darfield earthquake. A review of the ground motion records and geological setting indicates that the unfavorable interaction between fault rupture, radiation mechanism and complex geological conditions in the near-field region are main contributors to the earthquake damage. The analyzed near-source motions are shown to be made up of several sinusoidal pulses that are difficult for an empirical pulse indicator method to identify. Fourier analyses suggest that near-source pulse-type ground motions can excite basin natural vibration modes and generate large input energy demands related to the unexpected damages at the near field sites. Furthermore, a comparative assessment of the M_w 6.1 and M_w 7.0 earthquake recordings indicates that basin edge effects contributed to long-period ground motion components at 2~3s, coinciding with the range of resonance periods for the sedimentary deposits underneath Christchurch. The variation of both structural and geotechnical consequences and engineering relations with near-source and basin affects are discussed and compared with actual recordings and field observations. Results of this study improve the understanding of seismic hazards in the Christchurch, New Zealand region and risks to other cities located on sedimentary basins near earthquake sources.

Keywords: Near source affect, Christchurch Earthquake, Basin affect, Strong ground motions

1. INTRODUCTION

On February 22, 2011, an M_w 6.1 (USGS) earthquake struck the city and suburbs of Christchurch – the second largest city in New Zealand. Comparing with the nearby September 4, 2010 M_w 7.0 (USGS) Darfield earthquake, the Christchurch earthquake resulted in stronger ground shaking with a wider spread of liquefaction problems and structure damages (Cubrinovski et al. 2011). The most devastated area was the Central Business District (CBD). Despite severe damage to infrastructure, there were no deaths and only two injuries associated with the Darfield earthquake. In contrast, the Christchurch earthquake resulted in 181 deaths.

A review of the ground motion records and geological setting indicates that the unfavorable interaction between fault rupture, radiation mechanism and complex geological conditions in the near-field region are main contributors to the earthquake damage. This study provides a preliminary assessment of the ground motions recorded in the Christchurch area on February 22, 2011, especially on the examination of waveforms and spectral analysis to describe the physical relevance to engineering.

2. GEOLOGIC TECTONIC SETTING OF CHRISTCHURCH

The tectonic and geologic settings for the Christchurch area has been described in various studies (e.g., Barnhart et al., 2011; Bradley and Cubrinovski, 2011; Orense et. al., 2011), only aspects pertinent to this study are summarized here. Christchurch is located on the Canterbury Plain having subsurface materials generally consisting of 300 to 800+ m deep fan and river deposited sand, silt, and gravel underlain by sandstone and mudstone (Forsyth et al., 2008), as indicated in Fig. 1. The near surface soils are typically Holocene alluvial silt, sand, and gravel with the groundwater surface found 1m to

5m deep. Much of the Christchurch area was formed with estuarine, lagoonal, dune, and coastal swamp deposits and many engineered developments are located within recent reclaimed swamp lands. As evidenced by the outcome of the 2010 and 2011 earthquakes, much of these near-surface soils are liquefiable. The Port Hills within the Banks Peninsula, comprised of Tertiary basaltic rocks formed from now extinct volcanoes, lies along the southeast edge of Christchurch.

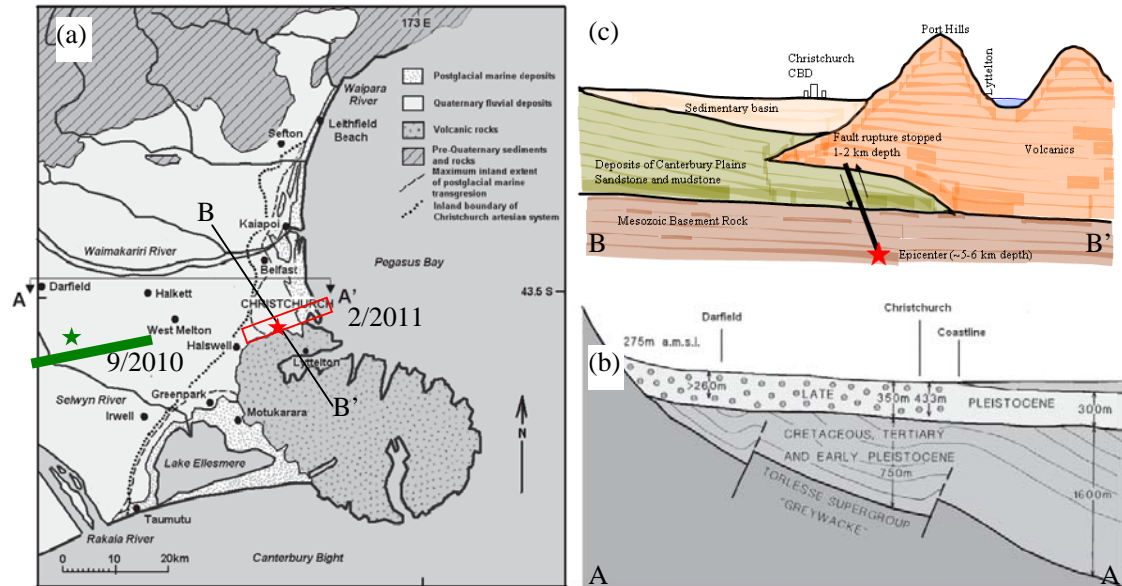


Figure 1. (a) Simplified geology of Christchurch region. The September 4, 2010 Darfield Earthquake and the February 22, 2011 Christchurch Earthquake fault rupture surface projection are identified by numerical dates, star identifies epicenter (locations are approximate). (b) Simplified soil strata along cross-section A-A'. {(a) and (b) are modified from Orense et. al. (2011)}. (c) Simplified cross-section B-B' showing epicenter, fault, and geologic section (not to scale).

On September 4, 2010 at 4:36 PM local time a M_w 7.0 (USGS, M_w 7.1 GNS) occurred on a previously unrecognized fault set having a hypocenter depth of about 5 km under the Canterbury Plain near Darfield about 30 km west of Christchurch. Figure 1a identifies the fault and epicenter approximate locations. This earthquake was associated with a complex fault rupture sequence involving several segments and rupture styles extending a length of about 29 km. Recorded motions in Christchurch ranged from peak ground accelerations (pga) generally between 0.18g to 0.25g. Portions of the near surface soils in Christchurch and surrounding area liquefied (Orense et. al., 2011). The aftershock sequence from the 2010 Darfield earthquake migrated east toward Christchurch (Barnhart et al., 2011).

At 12:51 PM local time on February 22, 2011, a moment magnitude M_w 6.1 (USGS; M_w 6.3 GNS) earthquake occurred 6 km south-east of the Christchurch CBD having a hypocenter at a depth of 5 to 6 km. This earthquake is located within the Darfield earthquake aftershock sequence. As show in Fig. 1c, the event involved a blind oblique-thrust rupture plane dipping about 67° to the south to a depth of about 7 km with a length of about 14 km extending east-northeast from Cashmere to the Avon-Heathcote estuary area (Beavan et al., 2011). It is a shallow fault with high friction and co-seismic stress drop, which produced highly directional seismic energy towards Christchurch city. The pga in the CBD was on average 0.5g in both the horizontal and vertical direction. The highest acceleration was recorded at Heathcote Valley Primary School, 1.7g in the horizontal direction and 2.2g in the vertical direction as reported by Bradley and Cubrinovski (2011), but differs from values reported herein due to processing methodologies. The earthquake rupture was characterized by a short duration, but severe shaking lasted over 20s at some locations on the sedimentary basin, which is a relatively long time for this earthquake size. The ground motions were very energetic relative to the fault rupture size, providing high-amplitude long-period motions well above that expected. Recordings show evidence that the sedimentary basin amplified the source ground motion waves and lengthened the shaking duration. Liquefaction was prominent in Christchurch (Cubrinovski, et al., 2011).

3. SEISMIC GROUND MOTION AND SPECTRUM ANALYSIS

Main shock Vol. 2 extended pass ground motion records from GeoNet (<http://www.geonet.org.nz/>) are used in this study. The published extended pass data were processed from Vol. 1 data using acausal filter of 0.05~25hz band pass. The authors would like to point out that by using the low-pass filter of 25 hz, the Vol. 2 data has smaller peak ground acceleration (sometimes significantly) compared to the pga provided in Vol. 1 data and reported by others (e.g., Bradley & Curbrinovski, 2011) who used a 50 hz low-pass filter for processing. Also the published Vol. 2 acceleration, velocity, and displacement time series are incompatible in the sense that straightforward integration of the acceleration time series will not reproduce the velocity and displacement time series that are provided to the public. This is most likely caused by the elimination of the zero padded portions from the acausal filters (Boore & Akkar, 2003). However, these variations due to filtering should not affect the analyses presented herein. Table 1 provides data on the six ground motion stations and recordings used in the present analyses, all at distances within 4km between the site and the fault surface projection (Rjb).

Table 1. Strong ground motion stations, peak recordings (obtained from GNS website), and results of pulse indicator analysis Baker (2007). FN and FP are fault normal and parallel components, F=False, T_w is wavelet period shown only for stations where pulse indicator analysis characterized a pulse.

Station Code	Station Name	Epic. Dist. (km)	Rjb (km)	Peak Acceleration (g)			Peak Velocity (cm/s)			Pulse Indicator/ T_w (s)		
				UP	Hor. 1	Hor. 2	UP	Hor. 1	Hor. 2	UP	FN	FP
LPCC	Lyttelton Port Company	5	4	0.4	0.8	0.9	16.6	37.0	41.5	F	3.9	F
HVSC	Heathcote Valley Primary School	2	1	1.5	1.5	1.2	39.2	97.3	62.3	F	F	F
PRPC	Pages Road Pumping Station	6	2	1.6	0.7	0.6	50.4	82.2	74.9	F	4.7	6.5
CMHS	Christchurch Cashmere High Sch.	6	1	0.8	0.4	0.4	13.9	42.1	46.0	F	F	F
CHHC	Christchurch Hospital	6	4	0.5	0.3	0.4	21.5	55.4	66.1	F	F	F
CCCC	Christchurch Cathedral College	5	3	0.7	0.5	0.4	21.3	71.4	51.5	F	F	1.6

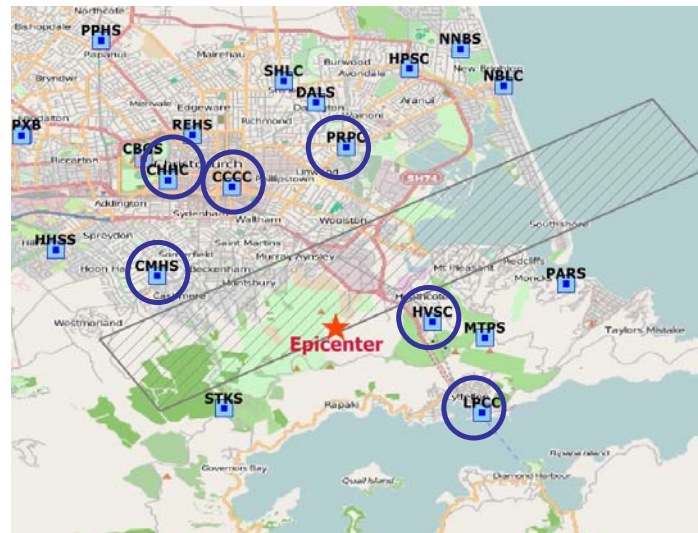


Figure 2. Strong ground motion station locations and fault slip plane per Beavan et al. (2011).

The Vol. 2 horizontal ground motions are rotated to the fault normal and fault parallel directions to examine the near fault rupture affect. Figure 2 shows the stations used to analyze the recordings for near source affects. The polygon delineates the approximate surface projection of the fault rupture plane modeled by Beavan et al. (2011). Their fault model shows the most significant fault plane slip distributions, providing the greatest contribution to the near-source ground motions, occur northeast of the epicenter. Beavan et al. (2011) reported a fixed fault plane geometry with strike 59° and dip 67° inferred from InSAR data, which is used herein as the basis for measuring the station azimuths. The azimuths are measured between the fault strike and the line joining each station perpendicular to the fault rupture. Figure 3 presents the fault-normal, fault-parallel, and vertical velocity time histories. As seen in Fig. 3, all six stations recorded large velocities. The wavelet algorithm developed by Baker (2007) is used in an attempt to quantitatively classify velocity pulses and determine the pulse period;

these results are shown in Table 1. Figure 4 presents the Fourier spectra for recordings shown in Fig. 3. In the present analysis the presence of near-source ground motion pulses and estimates of their period are identified by examining the recorded wave form time series and Fourier spectra, then comparing with the pulse indicator analysis results. The term near-source is used to describe pulse-like ground motion effects occurring from the fault rupture process. The following sections discuss various ground motion aspects observed in the recordings listed in Table 1, focusing more on observed wave forms and frequency signatures than on the motion amplitudes. The LPCC records are first examined for the near-source ground motion characteristics then compared with the HVSC recordings; both recorded on rock of differing shear wave velocity. These comparison results are then used to identify and compare near-source, basin, and site affects at stations PRPC, CMHS, CHHC, which are all recorded on the sedimentary basin shown in Fig. 1c.

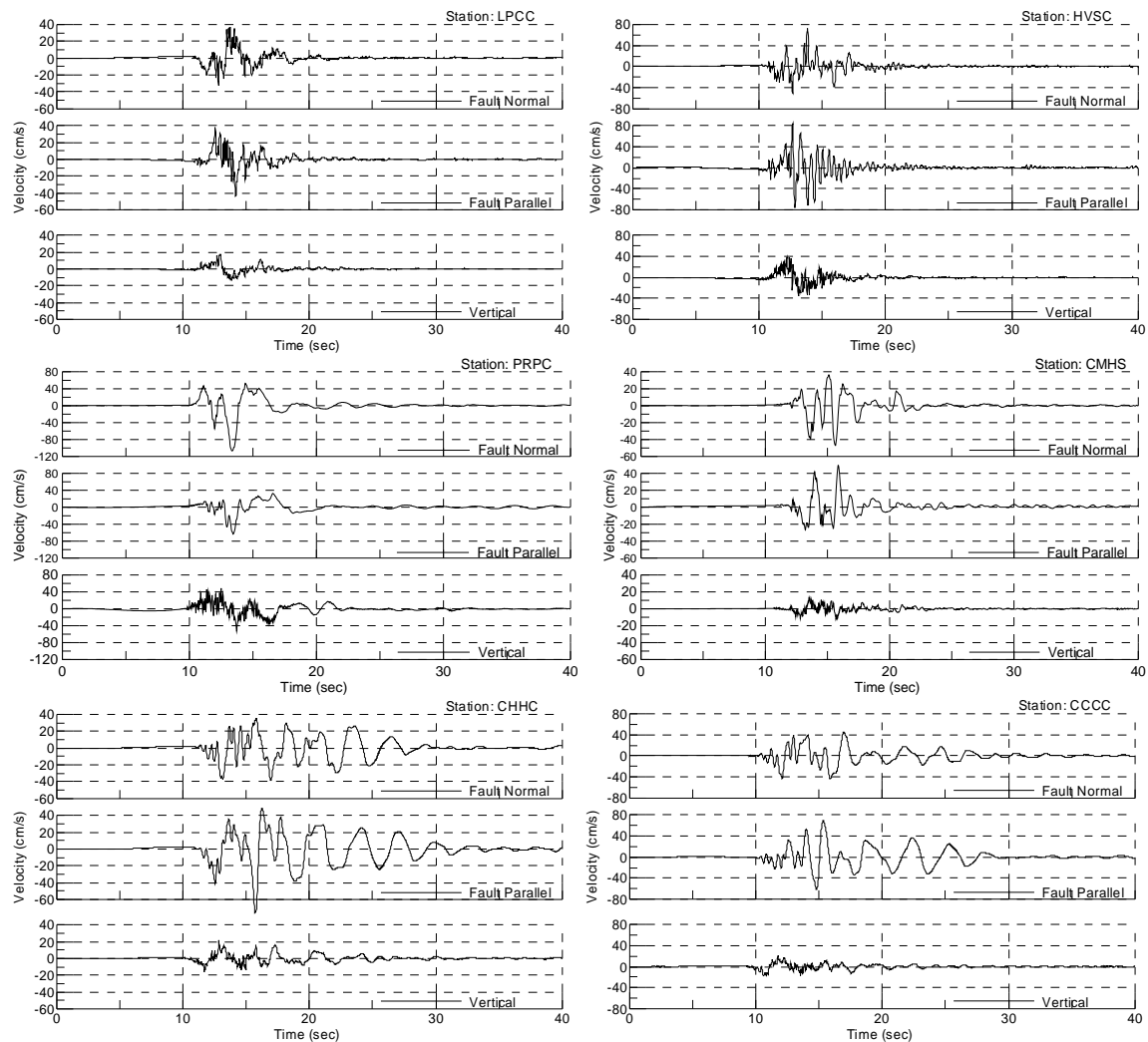


Figure 3. Velocity time histories recorded at stations LPCC, HVSC, PRPC, CMHS, CHHC, and CCCC. Note: vertical scale changes.

Table 2 presents a summary of periods that dominate the Fourier spectra for the selected records. These periods were selected from review of Fourier spectra and identifying the largest relative amplitude and tabulated in bins identified as A to T in Table 2. In some ranges the spectra contains a robust set of periods creating a mound shape around the peak periods identified in Table 2. For example, LPCC and HVSC identify fault normal peak periods at 3.3 and 3.6s, respectively which are accompanied by a broadband of motions covering periods from less than 2.5 to over 5s. Similar robustness is seen in the LPCC and HVSC fault normal component around 1.4s and fault parallel around 1.6s.

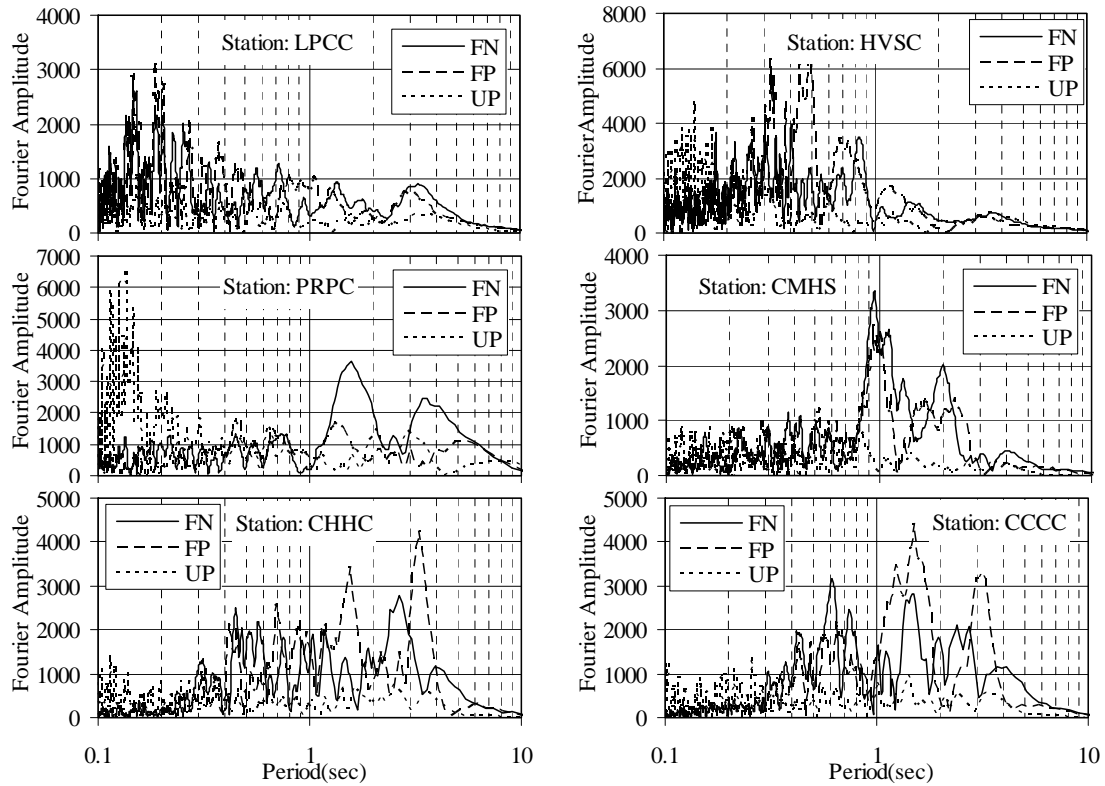


Figure 4. Fourier spectra for stations LPCC, HVSC, PRPC, CMHS, CHHC, and CCCC. Vertical scale changes.

Table 2. Dominant periods (sec) at selected stations from February 22, 2011 recordings, grouped in bins. Tan shaded columns distinguish source generated periods, basin natural periods in green, and blue identifies where source and basin periods coincide. See text for description.

	Sta/Bin	A	B	C	D	E	F	G	H	I	J	K	L	M	N	O	P	Q	R	S	T	
Fault Normal	LPCC			3.3				1.8	1.7	1.4				0.94			0.72			0.56	0.5	
	HVSC		3.6						1.6	1.4		1.1				0.84		0.70		0.56		
	PRPC		3.6	3.4		2.6				1.6								0.74			0.56	
	CMHS	4.0	3.7	3.1				2.0				1.3	1.1		0.95						0.58	0.52
	CCCC		3.7		2.7	2.4		2.0	1.5	1.4		1.1	1.0					0.74		0.62	0.58	
	CHHC		3.9			2.6	2.2	1.9		1.4	1.2		1.0	0.92				0.75		0.65	0.57	0.53
Fault Parallel	LPCC			3.2	2.8						1.2	1.1		0.92		0.80					0.53	
	HVSC			3.0					1.6		1.2						0.74	0.69				
	PRPC	4.8-5.5			2.9	2.5	2.2			1.4							0.74	0.67			0.55	
	CMHS						2.2	2.0	1.6				1.0	0.95					0.64	0.58	0.52	
	CCCC			3.2					1.5		1.2							0.74		0.65	0.57	
	CHHC			3.3		2.6	2.2		1.5		1.2			0.96	0.90			0.69		0.56	0.53	

4. NEAR SOURCE AFFECTS

The LPCC recording is on engineering rock (Bradley and Cubrinovski, 2011), with higher shear wave velocities than HVSC, and due to its site characteristics and close proximity the majority of strong shaking from this record is considered to be a composition of pulses directly related to the source rupture process, with limited influence from the propagation path and site conditions. The near-source pulses are clearly observable in the LPCC fault normal, fault parallel, and vertical velocity time histories of Fig. 3 and identified in Fig. 5. The estimated pulses are drawn in Fig. 5 overtop the original recording to identify their forms. As seen, for the most part the pulses take the form of a velocity sine wave or a Gaussian wavelet. However, the longest period pulse in the fault normal component of Fig. 5a can also be represented as a damped sine function or a Daubechies wavelet of order 4. Figs. 5a and 6 show how the first 3.3s of shaking in the LPCC recording for the fault normal component is made up of the superposition of several near-source pulses having periods identified in

Table 2. Figure 5a shows the 3.3 and 1.4s period wave pulses. Figure 6a diagrams the LPCC wave pulses with periods noted in Table 2. The initiation times for each pulse were selected through observation of the actual recording. The 3.3s pulse was assigned an estimated 20 cm/s amplitude and all others were scaled in proportion to their peak Fourier coefficient at the given period. Figure 6b shows that the superimposed waveform constructed from the pulses in Fig. 6a is a close match to the recorded motion. As a result, the near source motions can be represented by a decomposition of many different pulses related to the fault rupture process, but some of the pulses may not have any inference about the underlying fault rupture mechanics. The LPCC fault parallel and vertical motions can be evaluated similarly, but only the estimated form of the 3.3s period pulse is in Figs. 5b and 5c, respectively. Figure 5b shows little velocity at the beginning of motion, which may be represented by the superposition of waves of similar period but opposite sign initiating simultaneously. Figures 5d, 5e, and 5f show the near-source displacement wave forms for the LPCC recordings. These displacements will be compared to other stations, but due to space limitations displacements from other stations will not be plotted herein.

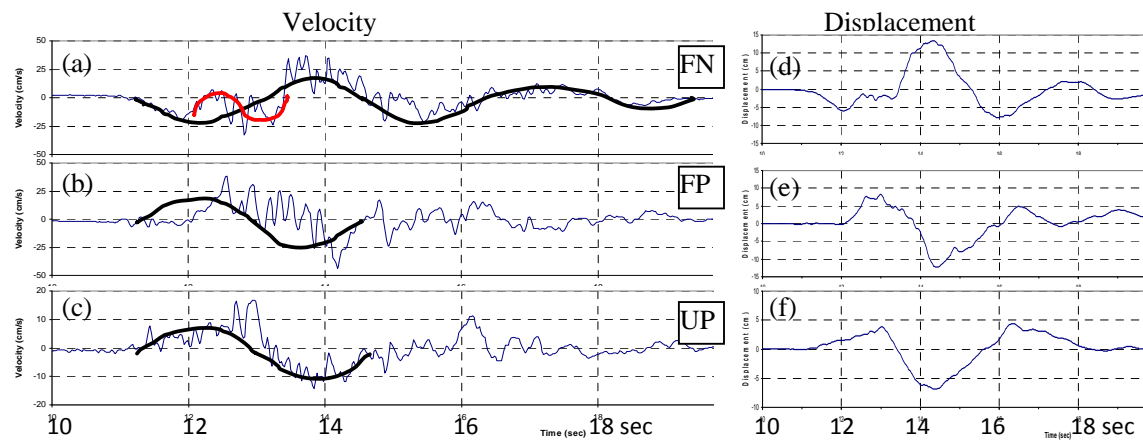


Figure 5. Velocity and displacement time series from station LPCC recorded on February 22, 2011 with marked estimated near-source pulses.

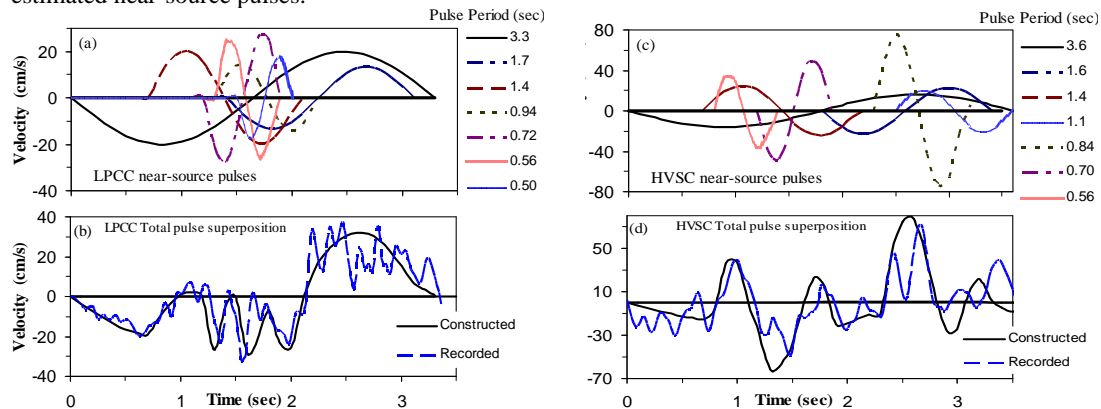


Figure 6. Near-source velocity pulses identified for the February 22, 2011 earthquake: Fault normal LPCC component: (a) identified pulses, (b) superposition of pulses in (a) compared to recording; Fault normal HVSC component: (c) identified pulses, (d) superposition of pulses in (c) compared to recording.

Review of the LPCC ground motion recordings identifies the following important engineering aspects:

- The ground motions are made up of several pulses having a sine wave form, most of them expected to be generated by the source fault rupture. The superposition of these sine wave pulses obscure some near-source characteristics in the raw and processed recordings.
- The significant near-source pulses have amplitudes ranging from 20 to 28 cm/s and long periods ranging from 0.56 to over 3.3s. The superposed peak amplitude is about 42 cm/s.
- LPCC oscillated in the fault normal direction at about a 3 to 3.3s period for several cycles.

- The vertical recording has a distinctive 3.3s pulse indicating the 3-D aspect of this transient.
- Displacement records show distinct near-source characteristic motions in all 3 components.
- The pulse periods identified in Fig. 6 are distinctly identified in the Fourier spectrum of Fig. 4.

In addition, an analysis was performed using the wavelet algorithm developed by Baker (2007) to help quantitatively characterize the ground motions containing strong velocity pulses, and to determine their periods; results are shown in Table 1. Baker (2007) recommends using the Daubechies wavelet of order 4 as a mother wavelet because he found it approximates the shape of many pulses, and therefore this was used in the analysis. Baker also assumes a minimum 30 cm/s amplitude. Using this method, only the LPCC fault normal component was classified as having a near source velocity pulse with a 3.9s period. The LPCC fault parallel and vertical motions were not classified as having near-source pulse-like motions. This is contradictory to the above stated findings and is most likely due to only the fault normal component having the combined superposition of all waves resulting in an oscillatory characteristic that closely matches the mother wavelet; whereas the combination of source pulses for the other two motions resulted in alternate shapes not matching the mother wavelet and/or amplitudes below minimum.

The above described characteristics associated with source generated pulses are distinguishable in other recordings. Table 2 shows many of the HVSC fault normal dominant periods are similar to those observed for LPCC. Those periods differing may be a result of source motions not reaching one of the sites or waves generated from path or local site affects. The wave amplitudes do change, sometimes significantly, between the LPCC and HVSC sites. This may result from differing proximity to the actual source generations, path, or site affects. The HVSC fault parallel and vertical periods are similarly comparable to the LPCC periods, with a few distinctions. The LPCC fault parallel component is more energetic in the 0.72 to 1.1s range and does not contain large amplitude pulses with periods between 0.5 and 0.7s, as opposed to the HVSC site. The wave forms in Fig. 3 identify similar near-source characteristics as previously described, especially in the HVSC vertical velocities. Figures 6c and 6d present the HVSC pulses and their superposition showing how the wave form can be reconstructed from the defined individual pulses. The 0.84s period pulse velocity reaches 75 cm/s. However, as indicated in Fig. 6d the superposition of pulses on the horizontal velocity recordings makes a “typical” near-source pattern difficult to distinguish; this is likely the reason why the Baker (2007) analysis method does not quantify the near-source motions in the HVSC recording, as indicated in Table 1. The HVSC displacement recordings also show distinctive patterns as identified in Fig. 5 for LPCC.

The analysis results shown in Figs. 5 and 6 allows several periods in Table 2 to be identified as likely to have been generated directly from the fault rupture process; these periods are tabulated in bins A, B, C, I, P, and S and highlighted in a tan color. Other periods in bins G and H may also be associated with pulses generated directly from the source, but from the data evaluated the results are uncertain.

The PRPC records in Fig. 3 show the distinctive near-source characteristics previously described and the Baker (2007) analysis also classified the two horizontal recordings as having near-source pulses with fault normal and parallel wavelet periods of 4.7 and 6.5s, respectively. These periods reach the upper end of those shown in Fig. 4. The PRPC horizontal displacement patterns are also consistent with the near-source motions, but are somewhat distorted possibly due to liquefaction induced near-surface ground movements in the region (Cubrinovski, et al., 2011).

The CMHS records show limited near-source characteristics and only in the fault-normal and vertical components observable in Fig. 4. The time series in Fig. 3 do not show discernable evidence of near-source motions, probably due to the site location being too far west of the significant slip distributions to receive any significant effect; as illustrated in the Beavan et al. (2011) fault model. CHHC and CCCC do show characteristics of near-source motions as previously described, but the superposition of horizontal pulses makes this somewhat difficult to discern. The vertical velocity clearly shows the motions and the Baker (2007) analysis is able to quantify the CCCC fault parallel component as containing near-fault motions with a 1.65s wavelet period. The displacement patterns

also match the near-source characteristics, but are somewhat distorted and a few components are indiscernible probably also due to liquefaction induced near-surface ground movements in the region (Cubrinovski, et al., 2011). Figure 3 shows large-amplitude long-period waves trailing the near-source pulses for many seconds. These motions are anticipated to be derived from basin-edge affects due to the geometry setting shown in Fig. 1. The basin affects, combined with site liquefaction, make the near-source affects more difficult to identify in the CHHC and CCCC records.

Two final comments on engineering observations of the near-source motions are made here. First, the near-source motions described herein dominate the first 3 or more seconds of shaking and for the most part are directly related to the peak velocities and displacements in all three motion directions. Peak horizontal and vertical accelerations also occur within this time of shaking and are significantly influenced by the near-source pulses. Second, Table 2 identifies very long near-source pulse periods which are unusual for this size of earthquake. Somerville (2003) and Baker (2007) indicate that near-source pulses from a M_w 6.1 to 6.3 earthquake would be expected to have periods in the range of 0.7 to 3.3s with a mean at 0.8 to 1.9s. The pulses identified in this study cover the expected range, but the longest periods of 5.5s far exceed that expected. The Darfield earthquake also experienced longer than expected periods. The nature of how these motions are generated needs to be better understood because they have strong engineering implications as described later.

5. BASIN EDGE AFFECTS

As previously indicated and shown in Fig. 1, Christchurch is located on a sedimentary basin overlying and west of the subsurface fault rupture. The source generated body waves enter the basin on its eastern edge and become trapped within the basin. The surface waves generated propagate across the basin significantly increasing the shaking duration and amplify long-period components within the ground motion. Previous studies (e.g., Bradley and Cubrinovski, 2011) attributed amplified ground motions in the CHHC, CCCC, and some other records stationed around the CBD (see Fig. 2) having periods of about 1.5 and 3.5s, directly to these basin affects, disregarding near-source pulses because they are not clearly evident in all the CBD records. Their assessment is in contrast with previous descriptions herein, and although the basin affects may amplify waves having periods in the 1.5 and 3.5s range the source affects should not be disregarded. This section identifies some interesting engineering implications and source-basin interactions.

The basin natural periods have been initially estimated for this study using recordings from the September 4, 2010 Darfield earthquake for each of the stations shown in Fig. 3. The four Darfield earthquake recordings CMHS, PRPC, CHHC, and CCCC made over the basin clearly identify basin natural periods of between 2.2 and 2.9s. In addition, the CHHC and CCCC records indicate a lower 3.3s vibration mode was also excited in the CBD area. The CMHS record indicates the basin at that section extends the natural vibration modes down to about 1.5s. The PRPC site also identifies natural vibration modes in the 1.3 to 2.0s period range. These period ranges in Table 2 are shaded in green and blue. Except at CMHS and PRPC, the Darfield motions in the 1.5s range at each of these stations are generally less significant than those having periods outside of the 1 to 2s range. This combined with the fact that the 1.4s pulses from the February 22, 2011 earthquake are clearly identifiable as source generated (see Figs. 5 and 6) indicates that the large amplitude waves at 1.4s period (Table 2 and Fig. 4), are a direct result of source generated pulses exciting the basin on which Christchurch is located.

The PRPC station shows significant fault normal ground motion amplification in Fig. 3 in the period range between 1.25 and 2.0s. As previously noted, the Darfield earthquake recordings at this station and orientation also showed an amplified response in the same period range, which is interpreted herein as a basin natural response mode. Apparently the broadband set of source generated pulses peaking at 1.4s period in the fault normal component (but ranging from about 1.2 to 2.0s) excited the basin natural vibration modes below the PRPC station resulting in the recorded large amplitude waves in this period range. Table 2 identifies the coincidence of source and basin periods. The CCCC fault parallel component has a similar response even though the Darfield motions did not indicate a natural mode in this period range.

The CHHC and CCCC records in Fig. 3 have long duration oscillations measuring between 2.3 and 3.3s that follow the near source shaking; these oscillations initiate after about the 15s mark on the recordings. The PRPC and CMHS records also show similar lower amplitude shorter duration oscillations. The near source motions previously described are identified as being very robust in the range of about 2.3 to over 5.5s. This means that the fault rupture process generated waves that excited the basin within this period range. Table 2 identifies the coincidence of the source and basin periods. Sections of the basin having natural vibration modes within this range would amplify the source generated motions explaining the large amplitude motions at periods greater than 2.3s that are shown for CHHC, CCCC, and PRPC. CHMS does not amplify motions greater than 2.2s because this station had little, if any, source generated excitation above the 2.2s period. PRPC, CHHC, and CCCC clearly recorded motions in the 0.74 and 0.56s range, which are shown in Table 2 as being source generated, but since the sections of basin (and site conditions) on which these stations reside apparently do not have a natural vibration mode at these periods, the motions were not amplified as they were for those above 2.3s.

6. LOCAL SITE AFFECTS

The local site affects in the February 22, 2011 earthquake were significant and dominated by liquefaction. The evidence of this site affect is identifiable in Fig. 4 for CHHC and CCCC where the horizontal lower period motions (i.e., those lower than 0.31s) are basically cut off. It has long been recognized that ground shaking can weaken soils and the weakening soils vibrate at longer periods, thus shifting the ground motion periods in Fig. 4 to the right. Aspects related to site affects are described in more detail by Bradley and Cubrinovski (2011). However, just as explained for the basin response to the source generated waves, the different sites throughout Christchurch would respond to waves affected by the source and the basin. If any site has a natural period, or shifts into a period, coincident with the source or basin generated wave periods, then the site amplifies the motions or sustains greater permanent deformations, which could be of great significance for large input waves.

7. MATHEMATICAL INTERPRETATION AND ENGINEERING IMPLICATIONS

The prior descriptions herein identify several ground motion observations that have important earthquake engineering implications and can be related to mathematical interpretation of sine pulse harmonics. Of most significance to the current study are the large amplitude pulses and oscillations covering a wide range of periods. These wide ranging motions provide a greater opportunity to excite natural vibration modes in engineered structures. Some examples on basin mode excitations at several sites from source pulses have been previously described. Similar to the basin and site vibrations, structural modes can also be excited independently or in combination with the source, basin, and site modes. Devastating motions can be generated when some or all of the source, basin, site, and structural modes coincide. This may explain some of the damages observed from the Christchurch earthquake, but detailed case studies are needed to verify.

An important engineering implication from the large-amplitude long-period motions are the modes contained within pulses such as those shown in Figs. 6a and 6c resembling a sine function. Figure 3 shows the basin generated oscillations at CHHC and CCCC as also having a sine harmonic function. Assuming these motions can be closely represented with a sine function, expansion as shown in Equation 1 identifies the multiple modes that make up the recorded motions (Tolstov, 1962, modified from page 36):

$$\left| \sin\left(\frac{2\pi}{T}t\right) \right| = \frac{2}{\pi} + \sum \left[\frac{4}{\pi} \frac{1}{1-n^2} \cos\left(n \frac{2\pi}{T}t\right) \right], \quad n = 2, 4, 6, \dots \quad (1)$$

Where T is the period, t is time, and n is the mode. Only even modes make up the expanded harmonics. For example, a source wave of period 3.0s and velocity amplitude of 20 cm/s can be expanded to show it consists of harmonics with periods of 1.5, 0.75, and 0.5, 0.375, 0.3s having respective amplitudes of 8.5, 1.7, 0.73, 0.40, and 0.26 cm/s. The amplitudes diminish rapidly, but large pulses as shown in Fig.

6c contain several modes of engineering significance.

Equation 1, and similar expansion forms for other harmonics and wavelets, identifies the importance of the large amplitude long period motions generated by source, basin, or site affects. As an example, Fig. 4 and Table 2 identify two robust broadband sets of source generated waves, the first having periods ranging from 2.3 to over 5.5s peaking around 3.0 to 3.6s (Set 1) and the second ranging from 1.2 to 2.0s peaking at 1.4s in the fault normal component (Set 2). These two pulse sets contain large amplitude pulses at 2.8 and 1.5s periods, respectively. Thus, the first mode ($n=2$) from Set 1 equals the source pulse period (1.4s) and constructively amplifies with the second pulse set. The second mode ($n=4$) of Set 1 and first mode ($n=2$) of Set 2 match the period of the 0.75s and constructively amplify with that source generated pulse. This process continues with higher modes from the longer period pulses. It may be coincidental that many of the different source generated pulses have the same modes. However, when the basin natural modes are in tune with the source generated pulses or their modes, then resonant response can result in damage to engineered structures. The PRPC record in Fig. 4 shows a large resonant response between 1.25 and 2.0s, which has apparent contributions from the pulse sets and their modes described above. As previously explained, similar wave amplification can result with site and structure response in combination with the basin and source generated waves. There are other examples from the February 22, 2011 earthquake that cannot be presented here due to space limitations. These effects are expected to have occurred at many locations throughout Christchurch and contributed to damages.

8. CONCLUSION

The February 22, 2011 near-fault recordings were shown to consist of several source pulses making up the wave form seen in the time series. The approximate pulse initiation times and amplitudes were estimated at the LPCC and HVSC stations and the pulse superposition were shown to match closely with recorded velocity waveforms. The sedimentary basin below Christchurch trapped and amplified waves, increasing the shaking amplitude and duration. The source generated pulses were shown to excite natural basin modes and amplify shaking at different stations. The superposition of multiple pulses in the near-field shows a high level of complexity in the Christchurch earthquake ground motions that may differ from many other near-source recordings. This makes existing quantitative methods (e.g., Baker, 2007) difficult to classify these near-source motions. Engineering implications related to long period source and basin generated waves were presented, identifying the importance of how modal aspects of these motions affect engineered structures. Further studies are needed to understand the uniqueness of near-source pulse decompositions and their interactions with geologic basins and local sites, and their impacts on engineered structures.

REFERENCES

- Baker, J.W. 2007. Quantitative Classification of Near-Fault Ground Motions. *BSSA* **97:5**, 1486-15011.
- Barnhart, W.D., M.J. Willis, R.B. Lohman, A.K. Melkonian. 2011. InSAR and Optical Constraints on Fault Slip during the 2010–2011 New Zealand Earthquake Sequence. *Seismological Research Letters* **82:6**, 815-823.
- Beavan, J., E. Fielding, M. Motagh, S. Samsonov, and N. Donnelly. 2011. Fault Location and Slip Distribution of the 22 February 2011 MW 6.2 Christchurch, New Zealand, Earthquake from Geodetic Data. *Seismological Research Letters* **82:6**, 789-799.
- Boore, D.M., and S. Akkar. 2003. Effect of causal and acausal filters on elastic and inelastic response spectra. *Earthquake Engineering and Structural Dynamics* 2003; 32, 1729-1748.
- Bradley, B. and M. Cubrinovski. 2011. Near-source Strong Ground Motions Observed in the 22 February 2011 Christchurch Earthquake. *Seismological Research Letters* **82:6**, 853-865.
- Cubrinovski, M., J.D. Bray, M. Taylor, S. Giorgini, B. Bradley, L. Wotherspoon, and J. Zupan. 2011. Soil Liquefaction Effects in the Central Business District during the February 2011 Christchurch Earthquake. *Seismological Research Letters* **82:6**, 893-904.
- Forsyth, P.J., Barrell, D.J.A., and Jongens, R. 2008. Geology of the Christchurch Area. GNS Science, NZ.
- Somerville, P.G. 2003. Magnitude Scaling of the Near Fault Rupture Directivity Pulse. *Phys. Earth Planet. Interiors* 137, No. 1, pp 201-212.
- Tolstov, G. P., 1962, "Fourier Series," Dover, New York.